Polym. Bull. (2011) 67:1443–1454
DOI 10.1007/s00289-011-0460-9

ORIGINAL PAPER

Polymer-assisted formation of hydrophobized, shape-anisotropic zinc oxide nanoparticles via an inverse emulsion technique

Christian Geidel · Kathy Schmidtke · Markus Klapper · Klaus Müllen

Received: 7 September 2010 / Accepted: 11 February 2011 / Published online: 23 February 2011

Abstract A one-step inverse emulsion process using amphiphilic surface-active copolymers for the synthesis of hydrophobized, shape-anisotropic inorganic nanoparticles is presented. While such structures are normally prepared sequentially by particle formation and hydrophobization, we have combined both reactions. This approach is demonstrated exemplarily with zinc oxide (ZnO) nanoparticles. A key issue is the design of amphiphilic copolymers that act as emulsifiers to enable an aggregate-free redispersion of the particles and to stabilize the inverse emulsion for the precipitation in the droplets. In a first approach, the stabilizing as well as the hydrophobizing property of the copolymers are combined with the ability to control the crystallization in one polymer (*s*tructure-*d*irecting *e*mulsifier—SDE). In a second approach, a mixture of two polymers is applied: an amphiphilic copolymer for hydrophobizing/stabilizing the inorganic nanoparticles and a polar or double hydrophilic polymer that induces the anisotropic growth of the ZnO nanocrystals (*s*tructure-*d*irecting *a*gents—SDA). Homopolymers and block copolymers, consisting of phosphonic acid groups or propylene oxide groups, were used as SDAs. Typically, hydrophobized shape-anisotropic particles of up to 600 nm in length and with an aspect ratio of 1:4 were obtained.

Keywords Zinc oxide · Anisotropic shape · Nanoparticle · Inverse emulsion · In situ hydrophobization

Electronic supplementary material The online version of this article (doi:10.1007/s00289-011-0460-9) contains supplementary material, which is available to authorized users.

C. Geidel · K. Schmidtke · M. Klapper (✉) · K. Müllen
Max Planck Institute for Polymer Research, Ackermannweg 10, 55128 Mainz, Germany
e-mail: klapper@mpip-mainz.mpg.de

Introduction

The controlled synthesis of inorganic nanocrystals or hybrid inorganic–organic materials with specific size is a rapidly developing field in science since physical and chemical properties, such as composite transparency [1] and catalytic activity [2], are strongly influenced by the shape of the nanoparticles [3].

One of the characteristics of nanomaterials is their large surface-to-volume ratio. It is important to modify the interfaces to prevent agglomeration of the particles or to incorporate them homogenously into polymer matrices [4]. There are few reports about synthesis and hydrophobization of inorganic NPs in a single step with low molecular weight surfactants. [5]. However, most of these particles have been synthesized by a two-step procedure, performing hydrophobization and synthesis of particles in separate steps [6, 7].

In addition to multi-step procedures and several transfers between different solvents, a second major drawback of this strategy is that the bonding between the low molecular weight surfactant and the particle surface is not strong enough to avoid desorption caused by high shear forces during the extrusion process [8].

To overcome both problems in the case of spherical inorganic nanoparticles, we have developed a versatile method which allows their preparation and hydrophobization in a single step using a precipitation process in an inverse emulsion. Amphiphilic copolymers play a central role [9–12]. In contrast to low molecular weight surfactants, these emulsifiers allow the use of higher precursor salt concentrations and act as multidenate chelating ligands, having a strong interaction with particle surfaces [13]. By systematic variation of the parameters in the applied inverse emulsion technique (e.g., emulsifier, ultrasonification treatment, polymer content), simple oxides, sulfides, or metals [9] as well as more complex inorganic materials, such as core-multiple-shell ZnO–silica polymer nanoparticles, have been synthesized [14].

Apart from size, shape can also be decisive for the properties of the nanomaterial [15]. ZnO has been used in solar cells [16], sensors [17], as activator for organic accelerators and as co-accelerator in the vulcanization process [18]. For these applications, the fabrication of morphologically distinct ZnO nanostructures is required. The shape-anisotropy of non-hydrophobized inorganic particles can be achieved by adding structure-directing agents (SDAs) that either act as templates [19] or selectively adsorb on certain crystal facets [20]. Consequently, this leads to an anisotropic crystallization of the inorganic material. As this process is typically applied only in aqueous media resulting in hydrophilic particles, the development of a simple and reproducible synthetic route of hydrophobized inorganic nanoparticles of specific size and shape remains a challenge.

We demonstrate exemplarily with ZnO a one-step inverse emulsion process capable of producing in situ hydrophobized, shape-anisotropic inorganic nanoparticles in the presence of either structure-directing emulsifiers (SDEs) or SDAs. As such, homopolymers, statistical as well as block copolymers, containing phosphonic acid groups or polypropylene oxide chains, are used in the particle formation process. They are applied alone or in combination with amphiphilic statistical copolymers acting as emulsifiers and the inorganic particle hydrophobizing agent.

Experimental

Materials

All reagents and solvents were purchased from commercial sources and were used as received unless otherwise stated. 2-(Ethylhexyl)methacrylate (EHMA, **M1**) and poly(ethyleneoxide)methacrylate (PEOMA, **M2**) were dried over calcium hydride and distilled before use. Copolymer **1** (PEHMA-*stat*-PPEOMA, $M_n = 10.700$ g/mol, PDI = 1.7, monomer ratio 95:5) was prepared by free radical polymerization, described elsewhere [14]. Poly(vinylphosphonic acid) (PVPA **3**–**5**) was synthesized according to reference [21] (Fig. 1).

Characterizations

NMR measurements were performed on a Bruker 250 MHz spectrometer. Gel permeation chromatography (GPC) versus poly(methyl methacrylate) (PMMA) standard was carried out at 30 °C using MZ-Gel SDplus 10E6, 10E4, and 500 columns, an ERC RI-101 differential refractometer detector, and tetrahydrofuran (THF) as eluent. SEM images were taken using a Zeiss Gemini 912 microscope. In the sample preparation for SEM, the nanoparticles dispersed in toluene were drop-cast on silica wafers. TEM images were obtained using a Technai F20 microscope or a Zeiss LEO 1530 Gemini microscope, and samples were prepared by drop-casting. The mean particle diameters were determined directly from each SEM/TEM image by measuring the diameters of 100 particles and averaging the values. Static light scattering experiments were carried out on an ALV Goniometer-System, ALV 7002 Muliple Tau Digital Correlator, He–Ne laser (632.8 nm) to identify the shape factor of the ZnO nanoparticles [22]. The XRD diagrams were measured in reflection mode (CuKα radiation) on a Philips powder diffractometer PW 1820.

Synthesis of the structure-directing emulsifier **2b**

For the synthesis of the monomer, 2-(diethoxyphosphory)polyethylene oxide methacrylate (DEP-PEOMA, **M3**), **M2** (30 mmol) was dissolved in 40 mL of dichloromethane (DCM). Triethylamine (21 mmol) and pyridine (12 mmol) were then added. The mixture was cooled to 0 °C before diethylchlorophosphate (22 mmol), dissolved in 5 mL of DCM, was slowly added over a period of 30 min. After stirring for 24 h at ambient temperature, the formed colorless precipitate was

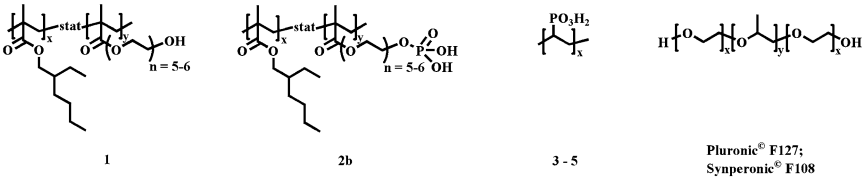

1 2b 3 - 5

Fig. 1 Applied polymers in the inverse emulsion technique

filtered off. The resulting solution was washed twice with 20 mL of saturated sodium chloride solution. After purification over a silica column (*n*-hexane:ethyl acetate = 2:1), **M3** remained as a colorless oil (70% yield). ^{1}H NMR (250 MHz, $CDCl_3$): $d = 1.29$ (tr, $POCH_2C\underline{H}_3$), 1.83 (s, $CO_2C\underline{H}_3CH_2$), 3.52 (s, $C\underline{H}_2C\underline{H}_2O$), 4.03–4.14 (m, $POC\underline{H}_2$), 5.46 (s, $CO_2CHC\underline{H}_2$), 6.0 (s, $CO_2CHC\underline{H}_2$). ^{13}C NMR (75 MHz, $CDCl_3$): 168.8, 137.6, 128.4, 67.3, 67.2, 64.0, 17.5, 16.3 ppm.

The copolymer poly(ethylhexyl methacrylate)-*stat*-poly (2-(diethoxyphosphory)polyethylene oxide methacrylate)) (PEHMA-*stat*-PDEP-PEOMA, **2a**) was prepared by free radical polymerization of **M1** (38 mmol) and **M3** (2 mmol) in 25 mL of toluene using mercaptoethanol (1 mmol) to adjust the molecular weight. The mixture was degassed by several freeze–pump–thaw cycles followed by flushing with argon. The reaction was carried out in a Schlenk flask sealed with a rubber septum at 70 °C using azobisisobutyronitrile (AIBN; 0.5 mmol) as initiator. The crude copolymer **2a** was precipitated twice from methanol and dried at room temperature under reduced pressure. ^{1}H NMR (250 MHz, $CDCl_3$): $d = 0.85$–2.0 (s, $C\underline{H}_3$, $C\underline{H}_2$, $C\underline{H}$), 3.8 (s, $CO_2C\underline{H}_2$), 4.1 (m, $POC\underline{H}_2C\underline{H}_3$). ^{13}C NMR (75 MHz, $CDCl_3$): 178.2, 177.8, 70.8, 70.3, 67.3, 45.3, 44.9, 38.6, 30.6, 29.1, 24.0, 23.1, 16.3, 14.1, 11.3 ppm. $M_n = 12200$ g/mol. PDI = 1.8. TGA = 362 °C (dec.).

The copolymer poly(ethylhexyl methacrylate)-*stat*-poly (2-((methacryloyloxy)polyethylene oxide) ethylphosphonic acid) (PEHMA-*stat*-PMPEOEPA, **2b**) was prepared by adding a 6-fold excess of trimethylsilylbromide to a 10 wt% solution of **2a** in DCM. The crude copolymer **2b** was precipitated twice from methanol and dried at room temperature under reduced pressure. ^{1}H NMR (250 MHz, $CDCl_3$): $d = 0.85$–2.0 (s, $C\underline{H}_3$, $C\underline{H}_2$, $C\underline{H}$), 3.8 (s, $CO_2C\underline{H}_2$), 4.5 (s, $PO\underline{H}$). ^{13}C NMR (75 MHz, $CDCl_3$): 178.2, 177.8, 70.8, 70.3, 45.3, 44.9, 38.6, 30.6, 29.1, 24.0, 23.1, 14.1, 11.3 ppm. TGA = 373 °C (dec.).[1]

Particle preparation

(1) Applying the SDE **2b**

Two solutions, each containing 100 mg of copolymer **2b** in 11.7 g toluene, were prepared. 1 mL of an aqueous solution of $Zn(Ac)_2$ (1.2 mol/L) was added to the first solution and 1 mL of an aqueous solution of NaOH (2.04 mol/L) to the second. All mixtures were stirred for 10 min at 500 rpm, followed by sonification (power 70 W) for 3 min, yielding stable emulsions. The first and second emulsions were combined and treated by ultrasound (power 70 W) again for 3 min. Water and toluene were evaporated at 70 °C under reduced pressure (120–180 mbar). The obtained solid was dried in vacuo (1×10^{-2} bar), washed with water to remove side products and other possible impurities, and dried in vacuo again. After freeze drying, the particles were redispersed by refluxing in toluene for 24 h.

(2) Applying structure-directing agents

Particle synthesis was performed in a modified manner as described above:

[1] Due to the amphiphilicity and the interaction of the deprotected copolymer with the gel of the GPC column, no reliable M_n could be obtained.

(i) Copolymer **1** (PEHMA-*stat*-PPEOMA) was used as emulsifier instead of copolymer **2b** (PEHMA-*stat*-PMPEOEPA) and
(ii) an additional emulsion containing an aqueous solution of SDA (1.2 g/L) was added to the $Zn(Ac)_2$ emulsion.

The synthesis and work-up followed the above-mentioned protocol.

Results and discussion

Inverse emulsion system

Based on the previously described synthesis of isotropic inorganic nanoparticles in an inverse emulsion of water dispersed in toluene [9], the simultaneous formation and hydrophobization of shape-anisotropic nanoparticles are performed in a single step. In contrast to the established strategy, polymers are added which combine the ability of stabilization and hydrophobization with structure directing properties.

Two strategies (Fig. 2) were studied for an inverse emulsion technique suitable for the preparation of shape-anisotropic in situ hydrophobized inorganic nanocrystals, using zinc oxide (ZnO) nanorods as samples.

Approach (i)—applying the structure-directing emulsifier **2b**

In approach (i), the synthesis of shape-anisotropic ZnO nanoparticles was performed by using two emulsions, containing a $Zn(Ac)_2$ and NaOH solution in toluene. They were stabilized by the SDE **2b** (PEHMA-*stat*-PMPEOEPA). The SDE simultaneously stabilizes the emulsion droplets, hydrophobizes the particle surface, and induces the anisotropic crystallization of the nanocrystals (Fig. 2, approach (i)).

In order to influence the crystallization of ZnO nanocrystals, the emulsifier 1 (PEHMA-*stat*-PPEOMA) was functionalized with a phosphonic acid group. This

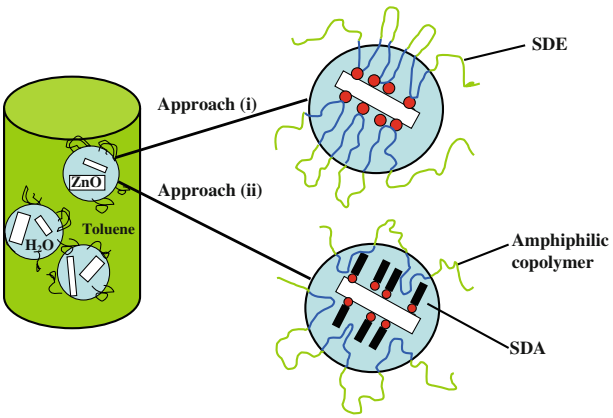

Fig. 2 Schematic view of the two strategies applied in the inverse emulsion technique

group was chosen for the low molecular surfactants influencing the crystallization of inorganic nanocrystals [23]. In case of ZnO it has been shown that surfactants, having e.g., carboxy [24] or citrate groups [25], influence the mineralization process. These anchor groups are responsible for raising the energy of some crystal facets relative to some other crystal facets. Consequently, this leads to anisotropic growth of the NPs. To further enhance this effect phosphonic acid groups were chosen, because it is known that they strongly interact with metal oxides [26].The protected monomer 2-(diethoxyphosphory)polyethylene oxide methacrylate (DEP-PEOMA, **M3**) was obtained by the reaction of **M2** with diethyl chlorophosphate (Fig. 3). The SDE poly(ethylhexyl methacrylate)-*stat*-poly (2-((methacryloyl-oxy)polyethylene oxide)ethylphosphonic acid) (PEHMA-*stat*-PMPEOEPA, **2b**) (M_n = 12.200 g/mol, PDI = 1.8, monomer ratio 90:10, Table 1) was obtained by the free radical polymerization of **M1** and **M3**, followed by deprotection with trimethylsilylbromide.

The DLS experiments proved that the SDE **2b** is capable of stabilizing a water/toluene emulsion. This amphiphilic copolymer was used as emulsifier in approach (i) following the protocol as described. The particles obtained were analyzed by X-ray powder diffractometry (XRD). The diffraction profile (Fig. 4a) showed all reflections of hexagonal ZnO (JCPDS card no: 36-1451) [27]. TEM experiments

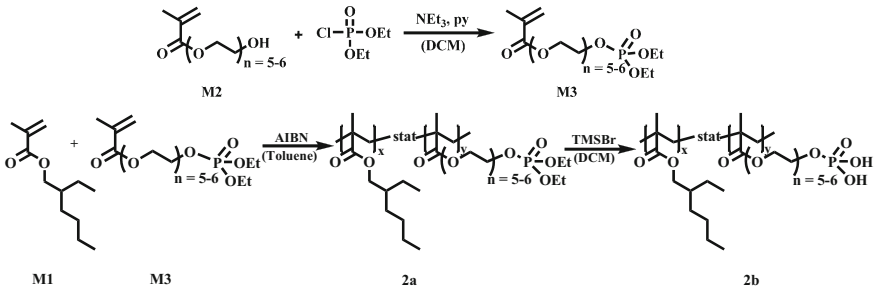

Fig. 3 Synthesis of the structure-directing emulsifier **2b**

Table 1 Applied structure directing polymers

Polymer	Composition			M_n (g/mol)	PDI
	x (mol%)	*y* (mol%)	*z* (mol%)		
PEHMA-*stat*-PMPEOEPA **2b**	10	90	–	12 200[b]	1.8
PVPA-1 **3**	100	–	–	62 000[a]	1.6
PVPA-2 **4**	100	–	–	44 700[a]	1.5
PVPA-3 **5**	100	–	–	35 500[a]	1.6
Pluronic© F127	37.5	25	37.5	12 600	–
Synperonic© F108	38.4	23.2	38.4	14 000	–

[a] Determined by SLS in 5 g/L aqueous NaH_2PO_4

[b] Determined by GPC with PMMA as standard

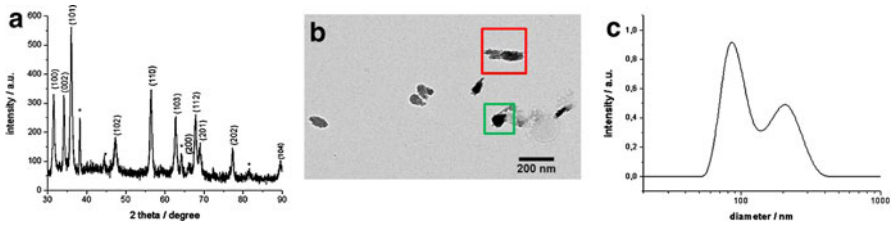

Fig. 4 **a** XRD pattern of ZnO nanocrystals using SDE **2b**. Asterisk indicates reflections of the aluminum support. **b** TEM images of ZnO nanorod dispersions using SDE **2b**, obtained after refluxing of the dried ZnO powders in 20 mL of toluene for 24 h. **c** DLS of ZnO NP dispersions, obtained by refluxing 32 mg dried particles in 20 mL toluene for 24 h

were then performed (Fig. 4b) to study the influence of the SDE on the crystallization.

Besides the rod-like (red square) morphology, smaller crystals (green square) were present. The strong interaction of the phosphonic acid groups with the ZnO surface led to a decreasing mobility of the hydrophilic monomer units in the course of the reaction, causing destabilization of the emulsion droplets. As a result, some confined nanoreactors coalesced, evident as smaller crystals in the TEM pictures. It is obvious that control of the crystal growth was achieved; however, spherical particles were still obtained. There was no further improvement of the shape-anisotropy, for example, by increasing the amount of phosphonic acid-containing monomers in the SDEs. Instead, an enhanced aggregation caused by a weaker hydrophobization of the particles occurred. This was further supported by DLS experiments. The size distribution of the dispersed hydrophobized ZnO NPs (Fig. 4c) indicated two maxima of 100 and 200 nm.

Approach (ii)—applying structure-directing agents

To overcome this drawback, we developed approach (ii) (Fig. 2), which is based on the use of two different types of polymers. One (copolymer 1) is in charge of the stabilization of the emulsion droplets while a second one (SDA) influences the crystal growth of the inorganic material.

In contrast to approach (i), the set up consists of three emulsions. The utilized emulsifier poly(ethylhexyl methacrylate)-*stat*-poly (poly ethylene oxide methacrylate) (PEHMA-*stat*-PPEOMA, **1**) was obtained by free radical polymerization of 2-(ethylhexyl)methacrylate (EHMA, **M1**) and poly(ethylene oxide methacrylate) (PEOMA, **M2**) (M_n = 10.700 g/mol, PDI = 1.7, monomer ratio 95:5) [14]. The previous study, dealing with spherical ZnO, CdS, and metals, has already shown that the use of **1** as emulsifier results in small particles and a narrow particle size distribution [11]. The first emulsion contains $Zn(Ac)_2$ and the second one a polymeric SDA. The addition of a third inverse emulsion containing sodium hydroxide in the water phase induces the precipitation of shape-anisotropic ZnO nanocrystals. During this process, the droplets of the three emulsions coalesce, and the sol–gel reaction takes place in confined emulsion droplets [10]. After the

resulting particles are washed, no peaks of side products, such as NaAc, or educts could be detected by X-ray diffractometry and IR analysis, as also observed previously for isotropic particles [9]. Besides the amphiphilic copolymer **1**, SDAs were applied in the inverse emulsion technique to induce shape-anisotropic growth of the ZnO nanocrystals.

Owing to the fact that the SDA, in contrast to the SDE, does not hydrophobize but assists the crystallization of the inorganic nanoparticles, we chose homopolymers **3**–**5**. Again, we selected polymers containing phosphonic acid groups (Table 1).

To study the influence of different molecular weights during the crystallization process, three poly(vinylphosphonic acids) **3**–**5**, varying in molecular weight, were synthesized and applied in the inverse emulsion technique. The solid products were analyzed by XRD. The diffraction profiles all showed reflections of hexagonal ZnO (JCPDS card no: 36-1451) [27]. TEM experiments were performed on all samples to determine the morphology of the synthesized nanocrystals (Fig. 5).

In all the cases, homogenously dispersed ZnO nanorods were obtained. No aggregation was observed. Validation of the size showed a particle length of 150–350 nm and a width of 50–90 nm. SLS investigations, exemplarily performed for the particles obtained by applying PVPA **3**, proved that the ZnO nanocrystals possess rod-like structures, which is indicated by a plateau in the Holtzer plot (see supporting information) [22]. TEM images reveal that the higher the molecular weight of the PVPAs the larger the particles obtained. This might be a result of the multidentate chelating effect of the SDA. At the beginning of the reaction, many crystallization centers are formed in one emulsion droplet [9]. Consequently, these "brickstones" are coordinated by the SDA which then merge together to build up the observed nanoparticles. The higher the M_n of the PVPA, the higher the number

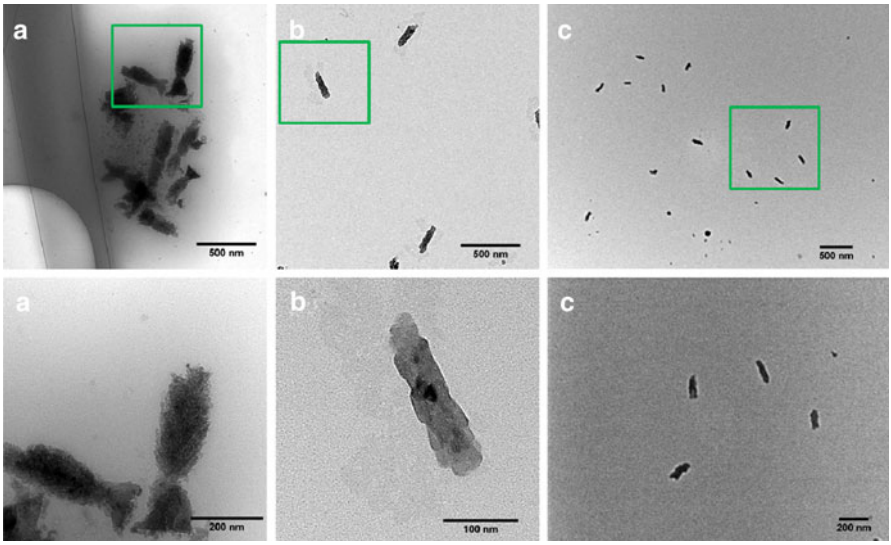

Fig. 5 TEM images of ZnO nanorod dispersions using **a** PVPA **3**, **b** PVPA **4**, and **c** PVPA **5** obtained after refluxing of the dried ZnO powders in 20 mL of toluene for 24 h

of coordinated crystallites and eventually the larger the ZnO nanoparticles will be. Furthermore, the nanorods not only differ in size but also in morphology. Double twin structures consisting of small crystallites were obtained by applying the PVPA **3** with the highest molecular weight. In contrast, using the low molecular weight PVPAs **4** and **5**, layered nanorod morphologies could be visualized by TEM experiments. It is possible to control the length and width as well as the morphology of ZnO nanorods by varying the molecular weight of the SDA. The topology of the nanocrystals using the PVPA **3** is similar to the nanorods obtained using SDE **2c**. By comparing both approaches (i, ii), it becomes noticeable that the second method allows better control of the crystallization of the inorganic nanoparticles. This is a result of the reallocation of the stabilizing/hydrophobizing and crystallization-influencing properties on two polymers. Other SDAs were applied to support this.

We chose double hydrophilic block copolymers (DHBCs) as they have shown excellent control in biomineralization of inorganic materials in many cases [28]. For example, poly(ethylene oxide)-poly(propylene oxide)-poly(ethylene oxide) (PEO-PPO-PEO) triblock copolymers, like the Pluronics, have been used as DHBC to assist the crystallization of inorganic as well as organic materials owing to the fact that the polypropylene groups interact selectively with certain crystal surfaces and therefore induce anisotropic growth [29–31].

The use of triblock copolymers in the inverse emulsion technique offers an amphiphilic environment with hydrophilic/hydrophobic domains in which the particles can grow. One should be able to control the linear growth of the nanorods by varying the block length.

We therefore investigated two triblock copolymers Pluronic F127 ($(PEO_{106}$-PPO-$_{70}$-$PEO_{106})$, $M_n = 12600$ g/mol and PEO/PPO = 3.03; Synperonic F108 (PEO_{122}-PPO-$_{56}$-PEO_{122}), $M_n = 14000$ g/mol and PEO/PPO = 4.36) with different PPO block lengths (Table 1). In the case of Pluronic F127, SEM and TEM (Fig. 6) clearly showed that the general morphology of the sample corresponded to flat-ended rods with an average length of 160 nm and a width of 100 nm (Fig. 6a). The hexagonal shape (Fig. 6b) indicated the wurtzite structure obtained by powder X-ray diffractometry (JCPDS card no: 36-1451) [27].

Using Synperonic F108 (PEO_{122}-PPO-$_{56}$-PEO_{122}), consisting of longer PEO chains, larger hydrophobized ZnO nanorods of 800 nm in length and 200 nm in width (SEM, Fig. 6c) were obtained. In comparison with the ZnO nanorods received with Pluronic F127, the rods became longer and revealed a rougher surface due to the

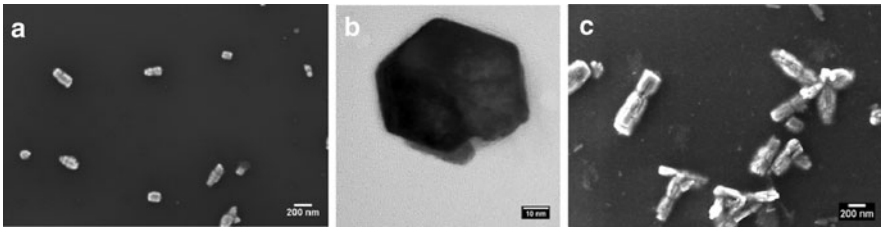

Fig. 6 SEM and TEM images of ZnO nanorod dispersions using **a/b** Pluronic F127 and **c** Synperonic F108, obtained after refluxing of the dried ZnO powders in 20 mL of toluene for 24 h

increase of the length of the PEO blocks by nearly constant PPO block. This is in good agreement with the literature proving that the ratio between the hydrophilic and hydrophobic part influences the crystal growth of hydrophilic CdS particles [31].

It has been proven that not only PVPAs but also triblock copolymers can influence the crystal growth in the inverse emulsion technique, which yields nanorods of different lengths and morphologies. In contrast to the particles obtained by the PVPAs, the surface is smoother, and the rod-like structures are built up of a double twin structure. In comparison to ZnO nanocrystals investigated by Wegner et al. [32] or Taubert et al. [33], the particles described here are much smaller (by a factor of 10) and redispersible in organic solvents, a prerequisite for incorporation into different polymer matrices (e.g., PEHMA, PMMA, or polystyrene) [10].

Conclusion

To date, a one-step procedure for synthesizing hydrophobized, shape-anisotropic inorganic nanocrystals has not been reported. We have now presented two very fast and efficient methods for obtaining hydrophobized ZnO nanorods based on the precipitation of inorganic particles in inverse emulsions in the presence of specially designed (co)polymers. In the first method, a combination of different polymers was used: an amphiphilic copolymer stabilized the emulsions while a water soluble polymer was applied in the aqueous droplets as SDA to control the crystallization process. In the second process, the amphiphilic copolymers acted as both emulsifiers and SDAs. In particular, commercially available PPO-containing block copolymers or easily accessible phosphonic acid-containing homopolymers as well as statistical copolymers were used simultaneously as stabilizers and SDAs. The choice of structure-directing polymers can control not only the shape of the ZnO nanorods obtained but also the size. The avoidance of a complex polymer synthesis makes the process attractive for industrial applications, especially when focusing on other systems such as nanocomposites. The emulsion process described here is anticipated to be adaptable for synthesizing other hydrophobic shape-anisotropic particles, such as cadmium sulfide nanocrystals. The homogeneous incorporation of such particles into a composite will not be a major challenge as we have previously [12] shown that the emulsifiers can be easily adopted to any polymeric matrix by varying the hydrophobic monomer in the amphiphilic copolymer. One can assume that new types of hybrid materials based on shape-anisotropic inorganic nanoparticles will become accessible.

Acknowledgments We gratefully thank Gunnar Glasser for the SEM images, Katrin Kirchhoff and Long Wang for the TEM images, Michael Steiert for powder diffraction and IAP for the financial support.

References

1. Althues H, Henle J, Kaskel J (2007) Functional inorganic nanofillers for transparent polymers. Chem Soc Rev 36:1454–1465. doi:10.1039/b608177k

2. Sarkar A, Mukherjee T, Kapoor S (2008) PVP-stabilized copper nanoparticles: a reusable catalyst for "click" reaction between terminal alkynes and azides in nonaqueous solvents. J Phys Chem C 112:3334–3340. doi:10.1021/jp077603i
3. Halbach TS, Thomann Y, Mülhaupt R (2008) Boehmite nanorod-reinforced-polyethylenes and ethylene/1-octene thermoplastic elastomer nanocomposites prepared by in situ olefin polymerization and melt compounding. J Polym Sci A 46:2755–2765. doi:10.1002/pola.22608
4. Kickelbick G (2003) Concepts for the incorporation of inorganic building blocks into organic polymers on a nanoscale. Prog Polym Sci 28:83–114. doi:10.1016/S0079-6700(02)00019-9
5. Wang X, Zhuang J, Peng Q, Li Y (2005) A general strategy for nanocrystal synthesis. Nature 437:121–124. doi:10.1038/nature03968
6. Koerner H, Kelley J, George J, Drummy L, Mirau P, Bell NS, Hsu JWP, Vaia R (2009) ZnO nanorod-thermoplastic polyurethane nanocomposites: morphology and shape memory performance. Macromolecules 42:8933–8942. doi:10.1021/ma901671v
7. Luna-Xavie JL, Guyot A, Bourgeat-Lami E (2002) Synthesis and characterization of silica/poly (methyl methacrylate) nanocomposite latex particles through emulsion polymerization using a cationic azo initiator. J Colloid Interface Sci 250:82–92. doi:10.1006/jcis.2002.8310
8. Meinders JM, Busscher HJ (1994) Adsorption and desorption of colloidal particles on glass in a parallel plate flow chamber—influence of ionic strength and shear rate. Colloid Polym Sci 272:478–486. doi:10.1007/BF00659461
9. Khrenov V, Klapper M, Koch M, Müllen K (2005) Surface functionalized ZnO particles designed for the use in transparent nanocomposites. Macromol Chem Phys 206:95–101. doi:10.1002/macp.200400213
10. Khrenov V, Schwager F, Klapper M, Koch M, Müllen K (2006) The formation of hydrophobic inorganic nanoparticles in the presence of amphiphilic copolymers. Colloid Polym Sci 284:927–934. doi:10.1007/s00396-006-1468-9
11. Klapper M, Clark CG Jr, Müllen K (2008) Application-directed syntheses of surface-functionalized organic and inorganic nanoparticles. Polym Int 57:181–202. doi:10.1002/pi.2301
12. Khrenov V, Klapper M, Koch M, Müllen K (2007) Compatibilization of inorganic particles for polymeric nanocomposites Optimization of the size and the compatibilty of ZnO particles. Polym Bull 58:799–807. doi:10.1007/s00289-006-0721-1
13. Chiad K, Stelzig SH, Gropeanu RA, Weil T, Klapper M, Müllen K (2009) Isothermal titration calorimetry: a powerful technique to quantify interactions in polymer hybrid systems. Macromolecules 42:7545–7552. doi:10.1021/ma9008912
14. Schmidtke K, Lieser G, Klapper M, Müllen K (2010) Complex inorganic/organic core-shell architectures via an inverse emulsion process. Colloid Polym Sci 288:333–339. doi:10.1007/s00396-009-2148-3
15. Jun YW, Choi JS, Cheon J (2006) Shape control of semiconductor and metal oxide nanocrystals through nonhydrolytic colloidal routes. Angew Chem Int Ed 45:3414–3439. doi:10.1002/anie.200503821
16. O'Reagan B, Schwarthz DT, Zakeeruddin SM, Grätzel M (2000) Electrodeposited nanocomposite n-p heterojunctions for solid-state dye-sensitized photovoltaics. Adv Mater 12:1263–1267. doi:0935-9648/00/1709-1263
17. Lin HM, Tzeng SJ, Hsiau PJ, Tsai WL (1998) Electrode effects on gas sensing properties of nanocrystalline zinc oxide. Nanostruct Mater 10:465–477. doi:10.1016/S0965-9773(98)00087-7
18. Versloot P, Haasnoot JG, Nieuwenhuizen PJ, Reedijk J, van Duin M, Put J (1997) Sulfur vulcanization of simple model olefins. Part V: double bond isomerization during accelerated sulfur vulcanization as studied by model olefins. Rubber Chem Technol 70:106–119
19. Tattershall CE, Jerome NP, Budd PM (2001) Oxyethylene/oxybutylene block copolymers as structure-directing agents in the preparation of mesoporous silica. J Mater Chem 11:2979–2984. doi:10.1039/B105484H
20. Yin Y, Alivisatos PA (2005) Colloidal nanocrystal synthesis and the organic–inorganic interface. Nature 437:664–670. doi:10.1038/nature04165
21. Bingöl B, Meyer WH, Wagner M, Wegner G (2006) Synthesis, microstructure, and acidity of poly(vinylphosphonic acid). Macromol Rapid Commun 27:1719–1724. doi:10.1002/marc.200600513
22. Schurtenberger P, Newman ME (1993) Characterization of biological and environmental particles using static and dynamic light scattering. Lewis Publishers, Boca Raton
23. Bao Y, An W, Turner CH, Krishnan KM (2010) The critical role of surfactants in the growth of cobalt nanoparticles. Langmuir 26:478–483. doi:10.1021/la902120e

24. Zhong X, Knoll W (2005) Morphology-controlled large-scale synthesis of ZnO nanocrystals from bulk ZnO. Chem Commun 9:1158–1160. doi:10.1039/b414948c
25. Tian ZR, Voigt JA, Liu J, Mckenzie B, Mcdermott MJ, Rodriguez MA, Konishi H, Xu H (2003) Complex and oriented ZnO nanostructures. Nat Mater 426:821–826. doi:10.1038/nmat1014
26. Frantz R, Durand JO, Granier M, Lanneau GF (2004) Triisopropoxysilyl-functionalized oxide nanoparticles using a di-*tert*-butyl phosphonate ester as the surface grafting agent. Tetrahedron Lett 45:2935–2937. doi:10.1016/j.tetlet.2004.02.076
27. Kihara K, Donnay G (1985) Anharmonic thermal vibrations in ZnO. Can Mineral 23:647–654
28. Cölfen H (2001) Double-hydrophilic block copolymers: synthesis and application as novel surfactants and crystal growth modifiers. Macromol Rapid Commun 22:219–252. doi:10.1002/1521-3927(20010201)
29. Burchard W (1983) Static and dynamic light scattering from branched polymers and biopolymers. Adv Polym Sci 48:1–124. doi:10.1007/3-540-12030-0_1
30. Lee WL, Cha SH, Kim KH, Kim BW, Lee J (2009) Shape-controlled synthesis of gold icosahedra and nanoplates using Pluronic P123 block copolymer and sodium chloride. Solid State Chem 182:3243–3248. doi:10.1016/j.jssc.2009.09.020
31. Yang CS, Awschalom DD, Stucky GD (2002) Growth of CdS nanorods in nonionic amphiphilic triblock copolymer systems. Chem Mater 14:1277–1284. doi:10.1021/cm011227b
32. Öner M, Norwig J, Meyer WH, Wegner G (1998) Control of ZnO crystallization by a PEO-*b*-PMAA diblock copolymer. Chem Mater 10:460–463. doi:10.1021/cm970450z
33. Taubert A, Glasser G, Palms D (2002) Kinetics and particle formation mechanism of zinc oxide particles in polymer-controlled precipitation from aqueous solution. Langmuir 18:4488–4494. doi:10.1021/la011799a